Scientific Journal of King Faisal University:
Basic and Applied Sciences

Performance Optimisation of a Wind Turbine Simulator with Transverse Cracked Blades using Taguchi-Based Grey Relational Analysis

Abdulhamed Hamdan Al-Hinai, Karu Clement Varaprasad and V. Vinod Kumar
Department of Mechanical and Mechatronic Engineering, Sohar University, Sohar, Oman

LINK	RECEIVED	ACCEPTED	PUBLISHED ONLINE	ASSIGNED TO AN ISSUE
https://doi.org/10.37575/b/eng/240044	24/09/2024	20/11/2024	20/11/2024	01/12/2024
NO. OF WORDS	**NO. OF PAGES**	**YEAR**	**VOLUME**	**ISSUE**
8039	8	2024	25	2

ABSTRACT

The presence of blade surface cracks creates chances for vibration propagation that affects wind turbine performance. This study examines the effects of transverse cracks on the vibration levels and power output of wind turbine systems. Multiple regression models are developed as predictive tools to highlight the impact of transverse crack sizes and variations in rotational speed on vibration levels and power generation. Grey relational analysis is used as an optimisation technique to identify optimal settings for maximum power output and minimum vibration levels. By modelling and analysing these factors, the study reveals a significant correlation between increased crack size and elevated vibration levels, which can compromise structural integrity. Additionally, while higher rotational speeds initially boost power output, they also lead to exponential increases in vibration, exacerbating the risks associated with blade defects. The findings emphasise the critical need for a balanced approach in optimising turbine performance, introducing a novel approach to speed management and vibration control, which is employed in this study. The research suggests potential avenues for future exploration, including the development of advanced materials and design innovations aimed at mitigating these risks, enabling safer and more efficient turbine operation.

KEYWORDS
Defect, optimal settings, power, rotational speed, regression, vibration

CITATION
Al-Hinai, A. H., Varaprasad, K. C. and Vinod Kumar, V. (2024). Performance optimisation of wind turbine simulator with transverse cracked blades using Taguchi-based grey relational analysis. *Scientific Journal of King Faisal University: Basic and Applied Sciences*, **25**(2), 42– 9. DOI: 10.37575/b/eng/240044

1. Introduction

Wind energy has rapidly gained prominence as a key renewable energy source, motivated by global implementation of energy efficiency and reliability (Wagner, 2015). The evolution of the wind energy sector from constant-speed wind turbine systems to more advanced systems reflects industrial innovation (Polinder, 2011). Direct-drive wind turbine systems are particularly valued for their reliability in wind turbine applications, especially as wind power is increasingly integrated into the grid (Blaabjerg and Ma, 2017).

Wind turbines are complex machines that convert wind energy into electrical power and are composed of key components such as blades, rotors and generators (Al-Hinai *et al.,* 2024). Horizontal-axis turbines are a more popular type and feature three blades and high-speed asynchronous generators (Lubosny, 2003). These systems rely on the dynamic wind pressure exerted on the blades to be converted into electrical energy. The efficiency of this process depends on the durability of the blades, which must withstand significant mechanical and environmental stresses (Pacheco *et al.*, 2024). However, blade defects remain a challenge, impacting turbine performance and longevity and leading to increased maintenance, downtime and safety risks (Liu *et al.*, 2015). Fatigue-related failures are common, particularly in blades and joints, with transverse fracture faults being a significant issue, as shown in Figure 1 (Sutherland, 1999). Crack formation in blades typically occurs in three steps: crack initiation, stable crack extension and eventual fracture. The total fatigue life of a blade can be expressed as the sum of crack initiation life and crack propagation life:

$$N_{total} = N_{initiation} + N_{propogation}$$

Wind turbine vibrations present significant challenges to the system's performance and longevity, originating from aerodynamic forces, mechanical imbalances and structural defects (Xie and Aly, 2020). Various control and vibration monitoring techniques are employed to detect and mitigate these issues (Barszcz, 2019). Experimental setups and simulations are vital for studying these vibrations and optimising turbine performance (Tibaldi *et al.*, 2016). Additionally, regression modelling and optimisation techniques are widely used in wind energy research to predict performance metrics in order to enhance efficiency (Balasubramanian *et al.*, 2020).

Figure 1: Transverse defects on wind turbine blades (Wang *et al.*, 2022)

This research seeks to optimise the wind turbine performance while minimising vibration levels. This involves an innovative analysis of a wind turbine simulation system with transversely defective blades operating at various rotational speeds. The study identifies the optimal settings that enhance power output while reducing vibration levels, making proactive maintenance through condition monitoring increasingly essential as wind turbines continue to grow in capacity (Koulocheris *et al.*, 2013). The structure of this paper is as follows: Section 2 reviews the existing literature on wind turbine technology and vibration challenges; Section 3 outlines the methodology used, including the simulation setup and data analysis techniques; Section 4 presents the results, focusing on the optimisation of power output and vibration reduction; and finally, Section 5 concludes with the study's contributions and suggestions for future research.

Corresponding Author: Abdulhamed Hamdan Al-Hinai 00968 99883473, 223306@students.su.edu.om

2. Literature Review

In recent years, wind energy has gained importance as a critical source of renewable energy. With advancements in wind turbine technology, the status of effective condition monitoring and vibration analysis has increased to ensure optimal performance and operational safety. As wind turbines become larger and are deployed in remote areas, condition monitoring becomes vital (Yang *et al.*, 2009).

Wind turbine blades are susceptible to various forms of damage and wear over time, leading to increased vibrations and decreased performance. Research has identified numerous technologies and methods to mitigate these vibrations and enhance wind turbine efficiency. Integrated approaches and optimisation algorithms have been explored extensively for vibration control and performance optimisation. Skrimpas *et al.* (2016) proposed an algorithm for effective along-wind vibration control of large wind turbines, demonstrating the potential of algorithmic solutions for dynamic response issues (Skrimpas *et al.*, 2016). Similarly, Sarkar and Chakraborty (2018) investigated optimal designs for long-wind vibration control, showcasing the synergy of advanced control algorithms and passive vibration control devices (Sarkar and Chakraborty, 2018).

Machine learning algorithms have also shown promise in structural health monitoring, as highlighted by Flah *et al.* (2020), who conducted a systematic review on the subject (Flah *et al.*, 2020). Conversely, Sheng (2012) focused on vibration analysis in the 'Wind Turbine Gearbox Condition Monitoring Round Robin Study', providing insights into the specific challenges and requirements of monitoring turbine gearboxes (Sheng, 2012). Liu *et al.* (2020) examined fault diagnosis of industrial wind turbine blade bearings using acoustic emission analysis, demonstrating its effectiveness in harsh conditions and slow-speed operations (Liu *et al.*, 2020).

Innovative methods continue to emerge. Joshuva and Sugumaran (2017) introduced a new blade condition monitoring technique based on the transmissibility of frequency response functions, utilising signals from multiple sensors for both damage detection and location (Joshuva and Sugumaran 2017). Ou *et al.* (2017) proposed a novel intelligent icing detection method for blades using SCADA data, addressing the significant issue of ice accretion (Ou *et al.*, 2017). Yang *et al.* (2015) emphasised the critical role of structural health monitoring and condition monitoring in assessing wind turbine components, while Antoniadou *et al.* (2015) discussed the complexities of damage detection in offshore wind turbines, highlighting the need for effective structural health monitoring and condition monitoring strategies (Yang *et al.*, 2015). Liu *et al.* (2019) explored non-contact methods such as thermography for blade icing detection, offering insights into subsurface damage detection (Liu et al., 2019). Florian and Sørensen (2015) stressed the need for reliable remote monitoring systems and proposed a blade lifetime assessment model for preventive maintenance planning (Florian and Sørensen 2015). Kusnick *et al.* (2015) focused on intelligent condition monitoring systems for rotor imbalance detection (Kusnick *et al.*, 2015).

Vibration analysis remains a cornerstone of wind turbine monitoring. Dong *et al.* (2018) studied structural vibration monitoring and operational modal analysis of offshore wind turbines, enhancing the understanding of vibration characteristics (Dong *et al.*, 2018). Liu *et al.* (2020) introduced an empirical wavelet thresholding method for blade-bearing fault detection, while Teng *et al.* (2019) proposed a novel vibration model for diagnosing compound faults in gearboxes (Liu *et al.*, 2020 and Teng *et al.*, 2019). He *et al.* (2016) developed an innovative order-tracking method for planetary gearbox vibration analysis (He *et al.*, 2016).

Blade defects significantly impact turbine performance and reliability. Manufacturing flaws are a primary cause of blade repairs and failures. Computational fluid dynamics can effectively analyse faults in vertical axis wind turbines, with defects affecting torque output. Researchers have developed probabilistic models to assess blade reliability, treating defects as uncertainty variables (Riddle *et al.*, 2018). Monte Carlo simulations describe failure probabilities, offering more accurate reliability assessments and potential reductions in design conservatism.

Despite extensive research on vibration analysis and condition monitoring, comprehensive studies on the performance of turbines with defective blades are lacking. Castorrini *et al.* (2019) conducted a computational analysis of performance deterioration due to environmental erosion, but more research is needed on defective blades' impact on overall performance (Castorrini *et al.*, 2019). Research focused on the aerodynamic shape optimisation of blades using advanced computational models and the development of novel optimisation algorithms, such as the artificial bee colony algorithm for shape optimisation (Derakhshan *et al.*, 2015). Non-stationary signal processing techniques applied to vibration analysis and the use of vibration and power curve analysis for detecting icing on blades represent potential areas for future research (Maheswari and Umamaheswari, 2017). As the wind energy industry expands, reducing operation and maintenance costs while improving reliability remains a priority (Tchakoua *et al.*, 2014).

3. Methods and Materials

To investigate the performance of a wind turbine simulator (WTS), real wind speed data from the town of Sohar in Oman was used as a hypothetical operating range of shaft rotational speed using WTS conversion. The WTS model employed in this research work was the SpectraQuest (SQ) type that used a VibraQuest (VQ) simulation software and data acquisition system. This investigation aimed to reduce the generated average of the vibration waveform range. This is basically the difference between the average of (m) positive peaks and the average of (n) negative peaks, as shown in Figure 2. When the vibration level was reduced, the WTS performance increased. The following equations were used to calculate the average of positive peaks, the average of negative peaks and the vibration level:

$$\text{Average of positive peaks} = \frac{\sum_{i=1}^{m}(\text{positive vibration peaks})}{m}$$

$$\text{Average of negative peaks} = \frac{\sum_{i=1}^{n}(\text{negative vibration peaks})}{n}$$

$$\text{Vibration level} = \text{average of positive peaks} - \text{average of negative peaks}$$

This section involved 1) an experimental setup of the SQ WTS; 2) the Taguchi design of the experiment (DoE); 3) experimental testing of the WTS as per DoE; 4) analysing the generated vibration waveform and power output; 5) analysing Taguchi response; 6) regression modelling of vibration level and power output; and finally 7) optimising the multi-responses using grey relational analysis (GRA) and sensitivity analysis.

Figure 2: Research concept

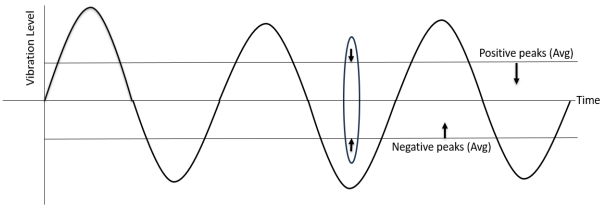

Experimental setup: The SQ WTS used in this research was of a three-blade type horizontal-axis wind turbine, as shown in Figure 3. The base dimensions were 2.991 m × 2.438 m, the centreline height was 2.369 m, the swept blade diameter was 3.3 m, and the weight was 222.7 kg. A tachometer and an accelerometer were mounted on the rotational shaft to measure the rotational speed and vibration level in one direction of vibrational excitation, respectively (Koulocheris *et al.*, 2013). A data acquisition system read the signals from these sensors and sent them to the VQ simulation software for analysis and to generate vibration reports, as shown in Figure 4. The three transversely defective blades used in this research work are shown in Figure 5.

Figure 3: SQ WTS

Figure 4: VQ analysis software

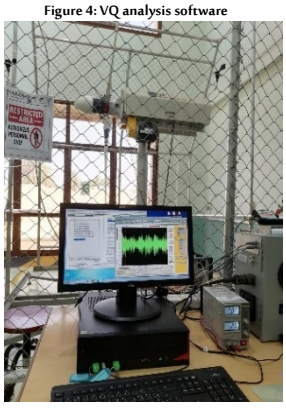

Figure 5: Three transversely defective blades (three crack levels)

Taguchi design of experiments: The experimental work was planned by Taguchi design of experiments (DoE) with two main independent parameters; namely A: crack size and B: shaft rotational speed. The transverse crack size varied from 33.4 mm to 74.0 mm, and finally to 98.8 mm, while the shaft rotational speed varied from 50 rpm to 100 rpm, and finally to 150 rpm, as a hypothetical operating range of Sohar wind speed using WTS conversion ratio. The total number of experimental tests performed was L9 (nine tests as per the DoE). The responses were the generated vibration level (average of positive peaks and average of negative peaks) and power output.

Experimental testing of the WTS as per DoE: This involved a systematic replacement of one of the three blades with transversely defective blades. The defective blades had crack sizes of 33.4 mm, 74.0 mm and 98.8 mm, respectively. The testing started with the first defective blade of 33.4 mm under a shaft rotational speed of 50 rpm, then 100 rpm, and finally 150 rpm. The same testing was repeated for defective blades of 74.0 mm and 98.8 mm, respectively.

Vibration waveform and power output analysis: The accelerometer read the vibration signals and sent them to the data acquisition system that transferred them to the VQ software to generate the vibration report in MS Excel format. The generated report showed a defined set of 10,000 vibration waves (positive and negative waveform peaks) for each test that were used later for vibration analysis. The WTS had a three-phase field-controlled alternator to produce the power output (voltage and current). The control interface of the WTS displayed both voltage and current that indicated the amount of field power output.

Regression modelling: The regression modelling for vibration levels and power output was performed to develop the following regression models; linear, linear and squared, linear and interaction, and finally the full model. The regression models were compared for the best fit with respect to the R-squared values for each response.

Optimisation of multi-responses using GRA: This research work aimed to optimise the performance of wind turbine systems while mitigating the vibration that occurs. For the average of negative vibration peaks and power output, the higher-the-better criterion was used, while for positive vibration peaks, the lower-the-better criterion was used. The normalisation of the original sequence of each response was calculated as follows:

For higher-the-better criterion: $$Y_{ij} = \frac{X_{ij} - min(X_{ij})}{max(X_{ij}) - min(X_{ij})}$$

For lower-the-better criterion: $$Y_{ij} = \frac{max(X_{ij}) - X_{ij}}{max(X_{ij}) - min(X_{ij})}$$

where x_{ij} is the measured response, $min(x_{ij})$ is the minimum of x_{ij} and $max(x_{ij})$ is the maximum of x_{ij}, i is the response variables and j is the experiment number. The deviation sequence (distinguishing coefficient) Δ_{ij} was calculated as follows:

$$\Delta_{ij} = max(Y_{ij}) - Y_{ij}$$

where $max(Y_{ij})$ is the expected sequence, Y_{ij} is the comparability sequence and Δ_{ij} is the deviation sequence of $max(Y_{ij})$ and Y_{ij}. The grey relational coefficient ξ_{ij} was calculated as follows:

$$\xi_{ij} = \frac{min(\Delta_{ij}) + \zeta \times max(\Delta_{ij})}{\Delta_{ij} + \zeta \times max(\Delta_{ij})}$$

where ζ is the differentiating coefficient, $0 \leq \zeta \leq 1$, and 0.5 is the widely accepted value. The grey relational grade (GRG) (γ_j) for each experiment was computed as follows, for n number of responses:

$$\gamma_j = \frac{\sum_{i=1}^{n} \xi_{ij}}{n}$$

If larger γ_j is obtained, then the equivalent set of process parameters is nearer to the most favourable optimal setting.

4. Results and Discussion

The generated vibration reports by the VQ software are discussed in this section, with regression analysis, optimisation and sensitivity analysis.

4.1. Initial Observations:

During the initial setup phase, preliminary observations were made to understand the baseline performance of the WTS with both healthy and defective blades. The presence of a transverse defect in one blade led to increased vibration levels and fluctuations in power output. These observations were important for this research work, as they showed the impact of blade defects under varying conditions:

- For healthy blade performance: The simulator with three healthy blades exhibited stable operational characteristics with minimal vibration levels. Power output increased consistently and within expected ranges for the given rotational speeds. The vibration waveforms recorded were smooth and showed almost no signs of irregularities, indicating the balanced and proper functioning of the blades.
- For defective blade performance: Replacing one healthy blade with a transversely defective blade resulted in noticeable changes. Increased vibration levels were immediately observed. There was a significant impact of the defect on the turbine's dynamic behaviour. The vibration waveforms displayed irregularities and higher peaks compared to the healthy blade setup, indicating the potential for structural instabilities. The power output was observed to fluctuate more with the defective blade. This reflected the impact of increased vibrations and possible energy losses.

4.2. Waveform Analysis Results:

The vibration signals were analysed and recorded using VQ software.

This software provides a detailed time-domain waveform for each test scenario. Figure 6 illustrates the vibration waveforms generated by VQ software. The vibration levels increased as the rotational speed increased.

Figure 6: Vibration waveforms: a) at 50 rpm (crack size = 33.4 mm), b) at 100 rpm (crack size = 33.4 mm), c) at 150 rpm (crack size = 33.4 mm), d) at 50 rpm (crack size = 74.0 mm), e) at 100 rpm (crack size = 74.0 mm), f) at 150 rpm (crack size = 74.0 mm), g) at 50 rpm (crack size = 98.8 mm), h) at 100 rpm (crack size = 98.8 mm), and i) at 150 rpm (crack size = 98.8 mm)

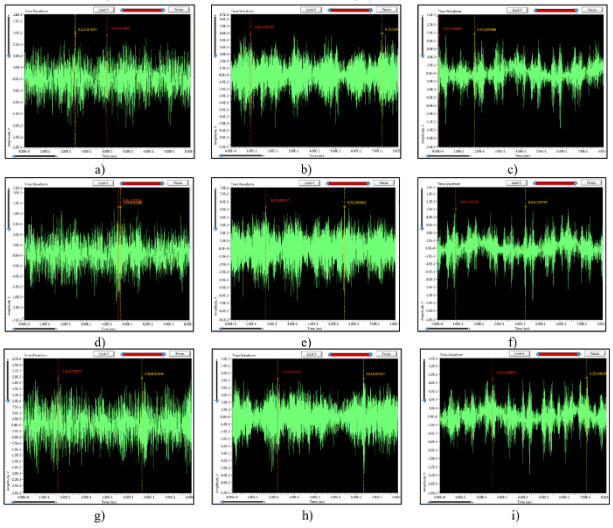

The detailed performance of the experimental work was performed for nine tests, considering the Taguchi design of the experiment. In each test, the VQ software generated a waveform report of a set of 10,000 vibration waves with positive and negative peaks. At the same time, the three-phase field-controlled alternator produced the power output (voltage and current) displayed on the control interface of the WTS. Table 1 shows the measured responses of the experimental work.

Table 1: Measured responses from experimental tests

	Input Parameters		Responses			
Tests	Crack Size, A (mm)	Rot Spd., B (rpm)	Avg. (negative peaks) (m/s^2)	Avg. (positive peaks) (m/s^2)	Vibration Level (m/s^2)	Power output (W)
1	33.4	50	-1.361	1.384	2.745	1.804
2	33.4	100	-4.990	4.647	9.637	9.912
3	33.4	150	-5.940	5.757	11.697	23.622
4	74.0	50	-1.337	1.470	2.807	1.539
5	74.0	100	-5.173	4.646	9.820	9.632
6	74.0	150	-6.105	6.116	12.221	23.331
7	98.8	50	-1.390	1.464	2.855	1.478
8	98.8	100	-5.171	4.750	9.921	9.475
9	98.8	150	-6.087	6.125	12.212	23.037

4.3. Taguchi Response Analysis:

Taguchi's response analysis focuses on optimising performance metrics through the design of experiments and the minimisation of variability. The experimental investigations on WTS with a transverse cracked blade were analysed using Taguchi's response analysis, response for means and response for signal-to-noise ratios (SNR). The influence of selected input process parameters on various performance measures such as average of peaks (negative and positive), vibration level and power output are detailed.

4.3.1. Taguchi's Response Analysis for the Average of Negative Peaks

In this case, the process parameters, crack size (A) and rotational speed (B), were analysed for their effects on the average of the negative side of vibration waveform peaks. In Table 2, the mean and SNR values illustrated how changes in each factor (A or B) impact the system's performance. Considering the higher-the-better criterion, the best possible set of process parameters observed from the analysis was A1B1, which means a crack size of 33.4 mm and a rotational speed of 50 rpm.

Table 2: Response table for the average of negative peaks

Level	Means		Signal-to-Noise Ratios	
	A	B	A	B
1	5.903	8.637	14.97	18.73
2	5.795	4.889	14.75	13.78
3	5.784	3.956	14.74	11.94
Delta	0.119	4.681	0.22	6.78
Rank	2	1	2	1

4.3.2. Influence of Process Parameters on the Average of Negative Peaks

Focusing on the average of negative peaks of the vibration waveform, it was observed that varying crack sizes had a small impact on the negative peak values. The mean values increased slightly from level 1 to level 3. This indicated that larger cracks resulted in slight increases in negative peak amplitudes. However, the variation in negative peaks associated with increasing the rotational speed is far more pronounced. As the rotational speed escalated from level 1 to level 3, negative peak values decreased significantly. This reflected a substantial negative correlation between higher rotational speeds and the average of negative peaks. The delta value of 4.681 further emphasised that rotational speed is considerably more influential on this response than the size of the crack.

4.3.3. Taguchi's Response Analysis for the Average of Positive Peaks

In this instance, the average of the positive side of the vibration waveform peaks was examined in relation to the process parameters of crack size (A) and rotating speed (B). The performance of the WTS was impacted by changes in each factor (A or B), as seen by the mean and SNR in Table 3. The optimal set of process parameters found in the analysis, while taking into account the lower-the-better criterion, was A1B1 also, which corresponded to a crack size of 33.4 mm and a rotational speed of 50 rpm.

Table 3: Response table for the average of positive peaks

Level	Means		Signal-to-Noise Ratios	
	A	B	A	B
1	3.930	1.440	-10.458	-3.162
2	4.078	4.681	-10.807	-13.407
3	4.113	5.999	-10.863	-15.558
Delta	0.184	4.560	0.406	12.396
Rank	2	1	2	1

4.3.4. Influence of Process Parameters on the Average of Positive Peaks

Examining the average of positive peaks of the vibration waveform, there was found to be a similar trend. The means showed a gradual increase from level 1 to level 3 as crack size increased. This suggested that larger cracks can lead to elevated positive peak amplitudes. However, the impact of rotational speed was once again more dramatic. The SNR declined steeply from level 1 to level 3. This indicated that higher rotational speeds correlate with significantly reduced positive peaks. The noticeable delta of 4.560 underscored how rotational speed influenced this parameter more strongly than crack size did, drawing parallels to the observed effects on negative peaks.

4.3.5. Taguchi's Response Analysis for the Vibration Level

The present study also examined the impact of two process parameters, namely crack size (A) and rotating speed (B), on the vibration waveform level. Table 4 shows how variations in each factor (A or B) affected the system's performance. Based on the lower-the-better criterion, A1B1, which indicated a crack size of 33.4 mm and a rotational speed of 50 rpm, was likewise the best feasible set of process parameters found in the analysis.

Table 4: Response table for vibration level

Level	Means		Signal-to-Noise Ratios	
	A	B	A	B
1	8.026	2.802	-16.604	-8.949
2	8.283	9.793	-16.850	-19.817
3	8.329	12.043	-16.926	-21.613
Delta	0.303	9.241	0.322	12.664
Rank	2	1	2	1

4.3.6. Influence Of Process Parameters on the Vibration Level

The vibration level analysis further reinforced the conclusion regarding the dominant role of rotational speed. As crack size increased, the average vibration level also rose. This suggested that larger cracks contributed to a wider level of vibration. The delta value of 0.303 indicated a consistent effect, but the influence of rotational speed was markedly more significant. With a delta of 9.241, the widening of the vibration level at higher speeds (from 2.802 to 12.043) highlighted that the increased rotational speeds led to substantial enhancements in the vibration profile, which correlated with the turbine's operational dynamics.

4.3.7. Taguchi's Response Analysis for the Power Output

The present study tested the impact of the two process parameters on the power output. The performance of the system was impacted by changes in each factor (A or B), as shown by the mean and signal-to-noise ratios values in Table 5. Considering the higher-the-better criterion, A1B3, which indicated a fracture size of 33.4 mm and a rotational speed of 150 rpm, was the best feasible set of process parameters found in the analysis.

Table 5: Response table for power output

Level	Means		Signal-to-Noise Ratios	
	A	B	A	B
1	11.779	1.607	17.505	4.088
2	11.501	9.673	16.925	19.710
3	11.330	23.330	16.725	27.358
Delta	0.449	21.723	0.779	23.270
Rank	2	1	2	1

4.3.8. Influence Of Process Parameters on The Power Output

When examining the generated power output, the effects of both parameters became even clearer. Here, as crack size increased, the power output consistently decreased. This indicated that larger cracks adversely impact energy production capability, which was illustrated by a delta of 0.449. In stark contrast, the influence of rotational speed was overwhelmingly positive. As rotational speeds rose, the mean power output surged dramatically, from 1.607 at level 1 to an impressive 23.330 at level 3, with a delta value of 21.723.

4.4. Analysis of Variance for Measured Performance:

Analysis of variance (ANOVA) is a statistical tool used to compare the means of input parameters to determine the significant differences between them. It assesses the observed variations in data due to real differences between input parameters. The ANOVA for the measured performance in WTS showed the significance of the input parameters, crack size (A) and rotational speed (B), on the system's responses. ANOVA was used on the performance measures at 95% confidence level and was computed using Minitab statistical software. In this context, ANOVA was likely to reveal that rotational speed (B) was the more dominant factor influencing both the vibration level and power output. Conversely, crack size (A) showed a statistically secondary role effect.

- For the average of negative peaks, the analysis revealed that crack size (A) had 2 degrees of freedom (DF) with an adjusted sum of squares (Adj SS) of 0.0261 and an adjusted mean square (Adj MS) of 0.0130. This yielded an F-value of 3.73 and a P-value of 0.122. In contrast, rotational speed (B) had 2 DF, an Adj SS of 36.8381, an Adj MS of 18.4190, an F-value of 5,270.03 and a significant P-value of 0.000. The error term was attributed to 4 DF and contributed an Adj SS of 0.0140 and an Adj MS of 0.0035. This brought the total Adj SS to 36.8781.
- For the average of positive peaks, crack size (A) also had 2 DF with an Adj SS of 0.0569 and an Adj MS of 0.0284. This resulted in an F-value of 2.65 and a P-value of 0.185. Rotational speed (B) exhibited a much larger effect, with 2 DF, an Adj SS of 33.0363, an Adj MS of 16.5181, an F-value of 1,538.58 and a P-value of 0.000. The error component again had 4 DF, yielding an Adj SS of 0.0429 and an Adj MS of 0.0107. This culminated in a total Adj SS of 33.1361.
- In the case of vibration range, crack size (A) was characterised by 2 DF, an Adj SS of 0.160 and an Adj MS of 0.0798. This led to an F-value of 4.69 and a P-value of 0.089. Rotational speed (B) highlighted a more substantial impact. It reflected in its 2 DF, an Adj SS of 139.328 and an Adj MS of 69.6642, which produced an F-value of 4,096.79 and a P-value of 0.000. The error term had 4 DF with an Adj SS of 0.068 and an Adj MS of 0.0170. This resulted in a total of 139.556 for the Adj SS.
- Lastly, for power output, crack size (A) held 2 DF with an Adj SS of 0.308 and an Adj MS of 0.154. This resulted in a significant F-value of 30.03 and a P-value of 0.004. Rotational speed (B)demonstrated an even stronger statistical significance, with 2 DF, an Adj SS of 723.471, an Adj MS of 361.736, an F-value of 70,470.46 and a P-value of 0.000. The error component contributed 4 DF with an Adj SS of 0.021 and an Adj MS of 0.005. This led to a total Adj SS of 723.800.

The ANOVA results demonstrated that rotational speed (B) was the higher significant factor influencing all the performance measures in the wind turbine simulator, with consistently high F-values and very low P-values across the board. While crack size (A) showed less influence, on the vibration level, it was mostly significant and, on the power output, it was more significant. However, its significance is considerable if the WTS run for a longer time.

4.5. Multi-Regression Modelling Results:

Regression is an effective statistical method used to model the relationship between dependent variables and independent variables. It helps to predict the dependent variable's value based on the known values of the independent variables. In this section, a regression analysis was conducted to quantify the relationship between crack size (A) and shaft rotational speed (B) as predictors and the average of negative peaks, average of positive peaks, vibration level and power output as responses. Using Minitab software in the regression analysis, four types of regression models were developed to determine the best model fit for WTS performance.

- The first model is a linear regression model that incorporates two input variables: crack size (A) and rotational speed (B).
- The second model, termed linear plus squared, not only includes the same linear input variables, A and B, but also adds squared terms for crack size (A^2) and rotational speed (B^2).
- The third model is a linear regression model with interaction, which includes the linear variables A and B alongside an interaction term that represents the product of crack size and rotational speed ($A \times B$).
- Lastly, the fourth model (full quadratic model) encompasses all the components of the previous models, integrating the linear variables A and B, their squared terms A^2 and B^2 and the interaction term $A \times B$. This comprehensive approach allows for a detailed exploration of how these variables collectively influence vibration range and power output.

The R-squared values of the developed models were compared to determine the best-fit model. The regression models analysed in the study yielded various R^2 values, which reflect the proportion of variance explained by the models across the outcomes:

- For the first model (linear regression model), the R^2 values were 89.203% for the average of negative peaks (in m/s^2), 94.279% for the average of positive peaks, 91.896% for the vibration range and 97.838% for power output.
- The second model (linear and squared) demonstrated a significant improvement, achieving R^2 values of 99.962% for average negative peaks, 99.870% for average positive peaks, 99.951% for vibration range and 99.997% for power output.
- The third model (linear and interaction) showed the R^2 values slightly lower but still substantial, with 89.217% for average negative peaks, 94.350% for average positive peaks, 91.931% for vibration range and 97.840% for power output.
- Finally, the fourth model (full quadratic), which incorporated linear, squared and interaction terms, attained R^2 values of 99.975% for average negative peaks, 99.941% for average positive peaks, 99.986% for vibration range and an impressive 99.999% for power output.

From the developed regression models, the full quadratic model showed the best fit. The regression equations for the responses are:

$$\text{Average of negative peaks} = 5.30860287 - 0.0042579A - 0.1580261B + 3.4165 \times 10^{-5}A^2 + 0.00056322B^2 - 2.082 \times 10^{-5}A \times B$$

$$\text{Average of positive peaks} = -3.7228 + 0.00262453A + 0.1193637B - 3.365 \times 10^{-5}A^2 - 0.0003848B^2 + 4.632 \times 10^{-5}A \times B$$

$$\text{Vibration level} = -9.0314029 + 0.00688248A + 0.27738983B - 6.781 \times 10^{-5}A^2 - 0.000948B^2 + 6.7141 \times 10^{-5}A \times B$$

$$\text{Power output} = -0.6459295 - 0.0032357A - 0.0039085B - 2.9461 \times 10^{-8}A^2 - 0.00111891B^2 - 3.634 \times 10^{-5}A \times B$$

4.6. Optimisation:

The objective of this research was to optimise the performance of the wind turbine system by balancing the power output and minimising vibration levels. The optimisation process utilised GRA in conjunction with a full factorial design in Minitab software. The optimisation process resulted in defining the optimal settings of process parameters. The GRA focused on two primary criteria: maximising the power output (higher-the-better) and minimising the vibration level (lower-the-better). In this case, the vibration level is the level between average of positive peaks and average of negative peaks. This means that only vibration level and power output responses are considered in the optimisation process. By applying these criteria, a grey relational grade (GRG) was computed for each experimental test.

- The first test received a Grade Relational Coefficient (GRC) of 1.000 and a GRG of 0.668, ranking it second overall.
- The second test reported a GRC of 0.407 and a GRG of 0.427, resulting in a seventh-place ranking.
- The third test, notable for its strong performance, achieved a GRC of 0.346 and a GRG of 0.673, earning the top rank of one.
- The fourth test recorded a GRC of 0.987 and a GRG of 0.661, securing the third rank.
- The fifth test had a GRC of 0.401 and a GRG of 0.421, placing it in eighth position.
- The sixth test yielded a GRC of 0.333 and a GRG of 0.654, ranking fifth overall.
- The seventh test obtained a GRC of 0.977 and a GRG of 0.655, which put it in fourth place.
- The eighth test had a GRC of 0.398 and a GRG of 0.418, finishing ninth.
- Finally, the ninth test achieved a GRC of 0.334 and a GRG of 0.642, resulting in a sixth-place ranking.

The GRG combined the GRCs into a single performance score. The third test (A1B3) showed the highest GRG (0.673), giving it the top rank, which means crack size = 33.4 mm and rotational speed = 150 rpm. This indicated the best overall performance. With higher GRG achieved, the third test was the best balance between vibration control and power output, making it a more optimal scenario. The confirmation of the results is shown in Table 6. The regression equation for GRG is:

$$\text{GRG} = 1.3724 + 2.3 \times 10^{-5}A - 0.018779B - 9.236 \times 10^{-8}A^2 + 9.46 \times 10^{-5}B^2 - 2.812 \times 10^{-6}A \times B$$

Table 6: Initial and optimal setting for WTS performance analysis

	Initial setting	Optimal setting
Parameters and levels	A1B1	A1B3
Average of negative peaks (m/s²)	-1.361	-5.940
Average of positive peaks (m/s²)	1.384	5.757
Vibration level (m/s²)	2.745	11.697
Power output (W)	1.804	23.622
Grey relational grade	0.668	0.673

4.7. Sensitivity Analysis:

To illustrate how the values of independent variables, the crack size and rotational speed, can affect the dependent variables, the vibration levels and power output, the analysis can be extended using theoretical frameworks grounded in the observed trends and relationships derived from the tested scenarios. Assumptions can be made as follows: 1) the relationship between independent variables and dependent variables can be approximated linearly in the feasible operational range; 2) crack size will vary between 0 mm (no defect) to 100 mm (severe defect), while rotational speed will vary from 0 rpm to 200 rpm, capturing both healthy operation and increasing operational stress; and finally, 3) vibration levels should be expected to increase with crack size and rotational speed, while power output should ideally increase with rotational speed but may decrease as crack size increases.

Based on observed data, a hypothetical model can be defined using the following generalised equations capturing the relationships between the variables:

$$Vibration\ level = c + (k1 \times crack\ size) + (k2 \times rotational\ speed)$$

$$Power\ output = d + (m1 \times rotational\ speed) - (m2 \times crack\ size)$$

Where k1, k2, m1 and m2 are coefficients representing the sensitivity of the respective dependent variables to the independent variables, and c and d are constants representing baseline vibration levels and power output under ideal conditions (e.g. no defect and no rotational speed). The differing signs in the equations captured the nuanced effects of each variable on the system's performance.

For simulated scenarios, to explore how the values of crack size and rotational speed affect vibration levels and power output, the following hypothetical values were considered:

- Crack size (mm): 0, 33.4, 50, 74, 98.8, 100
- Rotational speed (rpm): 50, 100, 150, 200

The following hypothetical coefficients were assumed based on the given data:

- k1 = 0.1 (increase of 0.1 m/s² for every mm of crack size)
- k2 = 0.05 (increase of 0.05 m/s² for every rpm of speed)
- m1 = 0.15 (increase of 0.15 W for every rpm of speed)
- m2 = 0.02 (decrease of 0.02 W for every mm of crack size)
- c = 1.5 (baseline vibration level with no defect)
- d = 5 (baseline power output with no defect)

Using these values, the vibration levels and power output were calculated. At a crack size of 0 mm and a rotational speed of 50 rpm, the vibration level measured 4 m/s², and the power output was recorded at 12.5 W. When the crack size increased to 33.4 mm and the rotational speed was set at 100 rpm, the vibration level rose significantly to 9.84 m/s², with the power output reaching 19.332 W. As the crack size continued to grow to 50 mm and the rotational speed increased to 150 rpm, the vibration level further escalated to 14 m/s², while the power output increased to 26.5 W. At a crack size of 74 mm and a rotational speed of 200 rpm, the vibration level was measured at 18.9 m/s², producing a power output of 33.52 W. Conversely, at a crack size of 98.8 mm and a rotational speed of 100 rpm, the vibration level recorded was 16.38 m/s², accompanied by a power output of 18.024 W. Finally, at a crack size of 100 mm with a rotational speed of 200 rpm, the vibration level peaked at 21.5 m/s², while the power output reached 33 W. These results illustrate the relationship between crack size, rotational speed, vibration levels and power output, highlighting the trends in performance as conditions change.

From the calculations in this simulated scenario, the relationship between independent and dependent variables can be observed clearly: as crack size increased, and/or as rotational speed increased, the average vibration levels tended to rise, and the power output initially increased with higher rotational speeds but was negatively influenced by increasing crack sizes. Thus, while higher speeds can enhance power generation, larger defect sizes could lead to a reduction in the overall power output. This theoretical exploration

allowed for anticipating the operational behaviour of the WTS under configurations, beyond those specifically tested, aiding in optimisation and fault management strategies.

4.8. Study's Limitations:

The use of wind speed data from Sohar, Oman, may restrict the generalisability of the results to other regions with different wind patterns. Additionally, the WTS may not fully capture the complexity of real-world turbine operations, which potentially affects the accuracy of vibration and power output measurements. The research focuses specifically on transverse blade defects and a limited range of parameters, such as crack size and shaft rotational speed. Other variables, such as wind turbulence and material fatigue, may be considered, which could influence the performance.

5. Conclusions

This research investigated the effects of input parameters such as crack size and rotational speed on the performance of a WTS system using vibration analysis, including regression analysis and the Taguchi design of experiments. The findings underscore the influence of blade defects on operational stability and power generation capabilities.

The experimental data revealed that the presence of defects significantly altered the vibration profile of the WTS. Specifically, the average of negative peaks increased from -1.361 m/s² for a healthy blade at 50 rpm to -5.940 m/s² when the crack size increased to 33.4 mm at 150 rpm. The average power output changed dramatically in tandem with these vibrations. This demonstrated increased fluctuations: the power output rose from 1.804 W (healthy blade at 50 rpm) to 23.622 W (transversely defective blade at 150 rpm).

Regression analysis yielded R^2 values of 99.999% for power output in the full quadratic model, the highest among all fitted models. This indicated an excellent fit and suggested that both crack size and rotational speed substantially contributed to the variance in performance metrics.

The optimisation process was undertaken using GRA, indicating that the optimal settings for enhanced performance were achieved with a crack size of 33.4 mm and a rotational speed of 150 rpm. This resulted in the best GRG of 0.673. These conditions effectively balance the power output (23.622 W) while maintaining a manageable vibration level (11.697 m/s²).

The sensitivity analysis demonstrated that both increasing crack size and rotational speed escalated vibration levels. At a crack size of 100 mm combined with a rotational speed of 200 rpm, vibration levels surged to 21.5 m/s², while power output was only marginally affected. This suggested operational strain could lead to mechanical failure over time.

This study lays a strong foundation for future research aimed at developing predictive maintenance strategies and improving the understanding of WTS under real-world conditions. Continuous monitoring and modelling of key parameters are essential for ensuring the reliability and efficiency of wind energy systems, reducing downtimes and optimising energy output in practical applications. Future research should focus on exploring advanced materials and design modifications to mitigate the adverse effects of cracks and enhance safe operation at higher speeds. Additionally, expanding on specific recommendations and addressing potential challenges in implementing these solutions will be critical for advancing the field.

6. Declarations

Ethical approval - The ethical approval declaration is not applicable.

Consent for publication - The authors consent to the publication of this manuscript.

Acknowledgement - The authors thank the Faculty of Engineering at Sohar University for their guidance.

Authors' contributions - A. H. A. designed the framework of this paper and was a major contributor to writing the manuscript. K. C. V. was a major contributor in revising and improving sections 1, 2 and 3. V. V. K. was also a major contributor to revising the manuscript and improving sections 4 and 5. All authors read and approved the final manuscript.

Conflicting interests - The authors declare that they have no competing interests relevant to this research paper.

Funding - This work did not receive any specific grant from funding agencies in the public, commercial or not-for-profit sectors.

Availability of data and materials - Materials used in this study are available upon reasonable request from the corresponding author.

Biographies

Abdulhamed Hamdan Al-Hinai

Department of Mechanical and Mechatronic Engineering, Sohar University, Sohar, Oman, +968 99883473 223306@students.su.edu.om

Al-Hinai was born in Oman, he received BSc in Mechanical Engineering from Sultan Qaboos University in Oman and M.Sc. in Thermal Power (Gas Turbine Technology) from Cranfield University in England. He is currently a Ph.D. research scholar at Sohar University in Oman. Abdulhamid has academic and administrative experience of more than 24 years. His research areas are Renewable energy Technologies, Wind Energy, Thermodynamics, and Solar Power. He attended and participated in many workshops, seminars, training courses and conferences.

ORCID ID: 0009-0005-5354-2895

Karu Clement Varaprasad

Department of Mechanical and Mechatronic Engineering, Sohar University, Sohar, Oman, +968 99808146, CKaru@su.edu.om

Varaprasad is an Indian associate professor in the Faculty of Engineering at Sohar University in Oman earned his Ph.D. in Mechanical Engineering from Jawaharlal Nehru Technological University, India in 2011. With over 20 years of teaching experience at various engineering colleges. Additionally, he is a member of the review team for the American Journal of Mechanical and Materials Engineering and serves on the editorial board of an international journal of mechanical, computational, and manufacturing research. He has contributed to over 23 reputable international journals.

ORCID ID: 0000-0002-8182-804X

V. Vinod Kumar

Department of Mechanical and Mechatronic Engineering, Sohar University, Sohar, Oman, +968 95979577, VKumar@su.edu.om

Vinod Kumar has been serving as an assistant professor and Program Coordinator of Mechanical and Mechatronic Engineering at Sohar University in Oman since 2009. He earned his Ph.D. in Mechanical Engineering from Nagpur University, India. With over 20 years of experience in academia, he has authored numerous research articles in internationally renowned journals and has also worked as a reviewer for various international journals. His research interests revolve around Passive Cooling, Energy Conservation, and Renewable Energy Technologies.

ORCID ID: 0000-0001-5420-4584

References

Al-Hinai, A., Varaprasad, K.C. and Kumar, V.V. (2024, June). Analytical Simulation Approach to Evaluate the Ambient Humidity Effects on the Performance of a Wind Accelerator. In *IOP Conference Series: Earth and Environmental Science*, **1365**(1), 012006. DOI: 10.1088/1755-1315/1365/1/012006

Balasubramanian, K., Thanikanti, S.B., Subramaniam, U., Sudhakar, N. and Sichilalu, S. (2020). A novel review on optimization techniques used in wind farm modelling. *Renewable Energy Focus*, **35**(n/a), 84–96. DOI: 10.1016/j.ref.2020.09.001

Barszcz, T. (2019). Standard Vibration Analysis Methods. In: T. Barszcz (eds.) *Vibration-Based Condition Monitoring of Wind Turbines. Applied Condition Monitoring*, Switzerland, Springer Nature Springer, DOI:10.1007/978-3-030-05971-2_2

Blaabjerg, F. and Ma, K. (2017). Wind energy systems. *IEEE*, **105**(11), 2116–31. DOI: 10.1109/JPROC.2017.2695485

Castorrini, A., Greco, E. and Sicilian, M. (2019). Computational analysis of performance deterioration of a wind turbine blade strip subjected to environmental erosion. *Computational Mechanics*, **64**(n/a), 1133–53. DOI: 10.1007/s00466-019-01697-0

Derakhshan, S., Tavaziani, A. and Kasaeian, N. (2015). Numerical shape optimization of a wind turbine blades using artificial bee colony algorithm. *Journal of Energy Resources Technology*, **137**(5), 051210. DOI: 10.1115/1.4031043

Dong, X., Lian, J., Wang, H., Yu, T. and Zhao, Y. (2018). Structural vibration monitoring and operational modal analysis of offshore wind turbine structure. *Ocean Engineering*, **150**(n/a), 280–97. DOI: 10.1016/J.OCEANENG.2017.12.052

Flah, M., Nunez, I., Ben Chaabene, W. and Nehdi, M.L. (2021). Machine learning algorithms in civil structural health monitoring: A systematic review. *Archives of Computational Methods in Engineering*, **28**(4), 2621–43. DOI: 10.1007/s11831-020-09471-9

Florian, M. and Dalsgaard Sørensen, J. (2015). Wind turbine blade life-time assessment model for preventive planning of operation and maintenance. *Journal of Marine Science and Engineering*, **3**(3), 1027–40. DOI: 10.3390/JMSE3031027

He, G., Ding, K., Li, W. and Jiao, X. (2016). A novel order tracking method for wind turbine planetary gearbox vibration analysis based on discrete spectrum correction technique. *Renewable Energy*, **87**(n/a), 364–75. DOI: 10.1016/J.RENENE.2015.10.036

Joshuva, A. and Sugumaran, V. (2017). A data driven approach for condition monitoring of wind turbine blade using vibration signals through best-first tree algorithm and functional trees algorithm: A comparative study. *ISA transactions*, **67**(n/a), 160–72. DOI: 10.1016/j.isatra.2017.02.002

Koulocheris, D., Gyparakis, G., Stathis, A. and Costopoulos, T. (2013). Vibration signals and condition monitoring for wind turbines. *Engineering*, **5**(12), 948. DOI: 10.4236/eng.2013.512116

Kusnick, J., Adams, D.E. and Griffith, D.T. (2015). Wind turbine rotor imbalance detection using nacelle and blade measurements. *Wind Energy*, **18**(2), 267–76. DOI: 10.1002/we.1696

Liu, X., Lu, C., Liang, S., Godbole, A. and Chen, Y. (2015). Influence of the vibration of large-scale wind turbine blade on the aerodynamic load. *Energy Procedia*, **75**(n/a), 873–9. DOI: 10.1016/j.egypro.2015.07.196

Liu, Y., Cheng, H., Kong, X., Wang, Q. and Cui, H. (2019). Intelligent wind turbine blade icing detection using supervisory control and data acquisition data and ensemble deep learning. *Energy Science & Engineering*, **7**(6), 2633–45. DOI: 10.1002/ese3.449

Liu, Z., Wang, X. and Zhang, L. (2020). Fault diagnosis of industrial wind turbine blade bearing using acoustic emission analysis. *IEEE Transactions on Instrumentation and Measurement*, **69**(9), 6630–9. DOI: 10.1109/TIM.2020.2969062

Lubosny, Z. (2003). Wind Turbine Generator Systems. In*: Z. Lubosny (eds.) Wind Turbine Operation in Electric Power Systems. Power Systems,* Berlin, Germany, Springer. DOI: 10.1007/978-3-662-10944-1_2

Maheswari, R.U. and Umamaheswari, R. (2017). Trends in non-stationary signal processing techniques applied to vibration analysis of wind turbine drive train–A contemporary survey. *Mechanical Systems and Signal Processing*, **85**(n/a), 296–311. DOI: 10.1016/J.YMSSP.2016.07.046

Ou, Y., Chatzi, E.N., Dertimanis, V.K. and Spiridonakos, M.D. (2017). Vibration-based experimental damage detection of a small-scale wind turbine blade. *Structural Health Monitoring*, **16**(1), 79–96. DOI: 10.1177/1475921716663876

Pacheco, J., Pimenta, F., Guimarães, S., Castro, G., Cunha, Á., Matos, J.C. and Magalhães, F. (2024). Experimental evaluation of fatigue in wind turbine blades with wake effects. *Engineering Structures*, **300**(n/a), 117140. DOI: 10.1016/j.engstruct.2023.117140

Polinder, H. (2011). Overview of and trends in wind turbine generator systems. In*: IEEE Power and Energy Society General Meeting*, Detroit, MI, USA, 24–28/07/2011. DOI: 10.1109/PES.2011.6039342

Riddle, T.W., Nelson, J.W. and Cairns, D.S. (2018). Effects of defects in composite wind turbine blades–Part 3: A framework for treating defects as uncertainty variables for blade analysis. *Wind Energy Science*, **3**(1), 107–20. DOI: 10.5194/wes-3-107-2018

Sarkar, S. and Chakraborty, A. (2018). Optimal design of semiactive MR-TLCD for along-wind vibration control of horizontal axis wind turbine tower. *Structural Control and Health Monitoring*, **25**(2), e2083. DOI: 10.1002/stc.2083

Sheng, S. (2012). *Wind turbine gearbox condition monitoring round robin study-vibration analysis* (No. NREL/TP-5000-54530). National Renewable Energy Lab. (NREL), Golden, CO (United States). DOI: 10.2172/1048981

Skrimpas, G.A., Kleani, K., Mijatovic, N., Sweeney, C.W., Jensen, B.B. and Holboell, J. (2016). Detection of icing on wind turbine blades by means of vibration and power curve analysis. *Wind Energy*, **19**(10), 1819–32. DOI: 10.2172/9460

Tchakoua, P., Wamkeue, R., Ouhrouche, M., Slaoui-Hasnaoui, F., Tameghe, T.A. and Ekemb, G. (2014). Wind turbine condition monitoring: State-of-the-art review, new trends, and future challenges. *Energies*, **7**(4), 2595–630. DOI: 10.3390/EN7042595

Teng, W., Ding, X., Cheng, H., Han, C., Liu, Y. and Mu, H. (2019). Compound faults diagnosis and analysis for a wind turbine gearbox via a novel vibration model and empirical wavelet transform. *Renewable Energy*, **136**(n/a), 393–402. DOI: 10.1016/j.renene.2018.12.094

Tibaldi, C., Kim, T., Larsen, T.J., Rasmussen, F., Rocca Serra, R.D. and Sanz, F. (2016). An investigation on wind turbine resonant vibrations. *Wind energy*, **19**(5), 847–59. DOI: 10.1002/WE.1869

Wagner, H. (2015). Introduction to wind energy systems. *EPJ Web of Conferences*, **98**(n/a), n/a. DOI: 10.1051/epjconf/20159804002

Wang, J., Zhang, L., Huang, X., Zhang, J. and Yuan, C. (2022). Initiation mechanism of transverse cracks in wind turbine blade trailing edge. *Energy Eng*, **119**(1), 407–18. DOI: 10.32604/ee.2022.016439

Xie, F. and Aly, A.M. (2020). Structural control and vibration issues in wind turbines: A review. *Engineering Structures*, **210**(n/a), 110087. DOI: 10.1016/j.engstruct.2019.110087

Yang, W., Lang, Z. and Tian, W. (2015). Condition monitoring and damage location of wind turbine blades by frequency response transmissibility analysis. *IEEE Transactions on Industrial Electronics*, **62**(10), 6558–64. DOI: 10.1109/TIE.2015.2418738

Yang, W., Tavner, P.J., Crabtree, C.J. and Wilkinson, M. (2009). Cost-effective condition monitoring for wind turbines. *IEEE Transactions on Industrial Electronics*, **57**(1), 263–71. DOI: 10.1109/TIE.2009.2032202